Thermo-mechanical, morphological and water absorption properties of thermoplastic starch/cellulose composite foams reinforced with PLA

Mohammad M. Hassan*[, a,d], Marie J. Le Guen [b,d], Nick Tucker [c,d,†], Kate Parker [b,d]

[a] Food & Bio-based Products Group, AgResearch Limited, Private Bag 4749, Christchurch 8140, New Zealand.

[b] Scion, 49 Sala Street, Rotorua 3010, New Zealand.

[c] Plant & Food Research, Lincoln Agricultural Research Centre, Gerald Street, Lincoln, Canterbury 7608, New Zealand.

[d] Biopolymer Network (BPN), 49 Sala street, Rotorua 3010, New Zealand.

***Correspondence to:**

Mohammad Mahbubul Hassan

Food & Bio-based Products Group, AgResearch Limited, Private Bag 4749, Christchurch 8140, New Zealand.

[†] Present address: School of Engineering, University of Lincoln, Brayford Pool, Lincoln LN6 7TS, U.K.

E-mail: mahbubul.hassan@agresearch.co.nz

Abstract

Expanded polystyrene foams are lightweight, cheap, and they have excellent strength and insulation properties. However, their inability to biodegrade in traditional landfill situations made their disposal problematic. Starch, a polysaccharide, has the potential to replace synthetic thermoplastics for some applications but starch-based foams are hydrophilic, which limits their applications. In this work, polylactide (PLA), a sustainably derived and industrially compostable polymer, was added to starch/cellulose composite foams to enhance their water barrier properties. PLA powder at various weight% was mixed with moistened starch and cellulose mixture, and composite foams were prepared by compression moulding at 220 °C. The thermomechanical and viscoelastic properties of the produced foam materials were analysed by thermogravimetric analysis, dynamic mechanical thermal analysis, mechanical testing, and also by the 3-point compressive mechanical quasi-static testing. It was found that the tensile strength of the composite foams increased with an increase in the PLA loading, which increased from 2.50 MPa for 0% PLA to 3.27 MPa for 9.72% PLA loading. The flexural strength also increased from 345.91 KPa for the 0% PLA to 378.53 KPa for the composite foam containing 4.86% PLA. The stiffness of the starch/cellulose composite increased with an increase of the PLA loading up to 4.86% PLA loading, and further decrease in PLA loading decreased the stiffness. The flexural modulus of the composite foams increased from 522 MPa for 0% PLA loading to 542.85 MPa for the 4.86% PLA loading. The thermal stability of the starch/cellulose composite foams also increased and the water absorbency decreased with the increased PLA loading.

Key words Biocomposite foams . Starch/cellulose composite foams . PLA . Rheology .

Introduction

Depletion of petrochemical resources, together with the accumulation of non-biodegradable plastics in the environment have led to renewed interest in the development of packaging from biomasses and other sustainable resources. Traditionally, cellulose and thermoplastic polymers have been used in the manufacturing of packaging. Although cellulose-based packaging materials (paper and cardboard) are sustainable alternatives to traditional thermoplastic polymeric packaging, they have many limitations, such as poor water barrier properties, that restrict their use in many applications. In addition, when they encounter water, they slowly lose their strength and finally disintegrate. On the other hand, most of the popular thermoplastic polymers currently used in packaging, such as low-density polyethylene (LDPE) and polypropylene (PP), are not biodegradable. Only a small percentage of plastic packaging is collected for recycling and therefore most of it is still ending up in a landfill, which pollutes our environment. Biodegradable plastics play an important role in this respect and they are increasingly replacing non-biodegradable and petrochemical-derived commodity plastics in packaging applications. The most promising synthetic biodegradable plastic is polylactic acid (PLA), which is made from corn by converting its starches to sugar, which is then converted to lactic acid (the monomer of PLA) through various fermentation stages (Rahman et al. 2011).

Starch, a natural fully biodegradable polysaccharide, is abundantly available at a very cheap price from potato, rice, wheat, corn, tapioca, cassava, and other crops. When moistened

starch is heated under shear, it loses its crystallinity and thermoplastic starch is produced. With the addition of a plasticiser, it can be processed like synthetic plastics using traditional plastic processing machinery, such as injection moulding (Swanson et al. 1993; Stepto 2006; Soukeabkaew et al., 2015). Unfortunately, thermoplastic starch produced from native starch exhibits low mechanical strength and poor water barrier properties, which severely limit its application (Dos Santos et al. 2018). A range of fibrous materials and clays including β-carotene (Kim and Huber 2016), nanoclay (Romero-Bastida et al. 2016), kaolinite (Mbey and Thomas 2015), sugarcane bagasse fibres (Dos Santos et al. 2018), flax fibres (Romero-Bastida et al. 2016), date palm fibres (Ibrahim et al. 2017), jute fibres (Wang et al. 2017; Soykeabkaew et al., 2015; Soykeabkaew et al., 2004), cellulose nanocrystals (Ali et al. 2018; Tabassi et al. 2016), β-glucan (Sagnelli et al. 2017), wheat gluten (Muneer et al. 2015), sugar palm fibres (Edhirej et al. 2017), and cellulose nanowhiskers (Liu et al. 2017), has been investigated to enhance its mechanical properties. The blending with various natural and synthetic polymers, such as zein (Corradini et al. 2006), chitosan (Mendes et al. 2016), natural rubber (Carmona et al. 2014), and the aliphatic polyester (Martin et al. 2001), has been investigated for the same purpose.

Foam packaging is very popular because of its ultra-lightweight and good thermal insulation properties. For example, non-biodegradable expanded polystyrene (EPS)-based foam packaging is extensively utilised for hot and cold food packaging due to its low cost. Thermoplastic starch-based foams have also been investigated for packaging applications as they have thermal insulation properties comparable with currently used EPS foams (Deng and Catchmark 2014; Zhou et al. 2006; Glenn et al., 2001a). However, starch foams behave differently as moisture conditions vary because of their high hydrophilicity (Glenn et al. 2001b). At high humidity or in contact with water, they lose strength, shape and structural integrity (Shogren et al. 1998). Conversely, at low humidity conditions, they lose their plastic

properties and become brittle. It was found that the increase in amylose content in the starch produces denser and stronger foams with a sacrifice in flexibility (Noorbakhsh-Soltani et al., 2018). On the other hand, starch with high amylopectin content produces light-weight foams but with poorer strength (Lawton et al., 1999). The addition of microfibrillated cellulose to starch also has been extensively investigated to make the starch-made materials strong (Kaushik et al. 2010; Hietala et al. 2013; Spiridon et al. 2014). The application of various plasticisers including glycerol has decreased the brittleness of starch-based materials (Avérous et al. 2000; Ghanbari et al. 2018). Sometimes, they are coated with a thermoplastic polymer to improve their water barrier properties. However, if holes are formed on the surface of the thermoplastic coating, their water barrier properties are compromised. Natural rubber latex has been extensively investigated to improve the barrier properties of starch-based foams (Subramaniam 1990).

PLA is a hydrophobic polymer that fully degrades under certain conditions (Ghorpade et al. 2001). Cellulose fibre, microfibrillated cellulose, cellulose nanocrystals, and PLA have been investigated as a reinforcing agent for the strengthening of starch-based films and foams [Patil et al., 2016; Shirai et al., 2013, Soykeabkaew et al., 2012]. The addition of microfibrillated cellulose to starch and crosslinking them by the 1,2,3,4-butane tetracarboxylic acid enhanced the strength of the produced cellulose-reinforced starch films [Patil wet al., 2016]. Shirai et al. reported the reinforcement of citrate and adipate ester plasticised starch films by the addition of PLA, which exhibited tensile strength in the range of 0.6 to 1.3 MPa [Shirai et al., 2013]. The addition of PLA to tapioca starch in the presence of glycerol and other plasticisers increased the tensile strength and moisture barrier properties, and decreased the moisture content of the produced foam [Preechawong et al., 2005]. Cellulose reinforced starch foam-based packaging has already been marketed by Earthpac and Paperfoam as an alternative to paper-based packaging, but their very poor water

barrier properties make them unsuitable for the replacement of hydrophobic EPS foam packaging.

It is known that PLA films have considerably higher moisture barrier properties compared to starch films [Muller et al., 2016] but it was not considered for the enhancement of strength and barrier properties of starch/cellulose composite foams. Therefore, we envisaged that the addition of PLA to potato starch/cellulose composite foam not only would enhance its strength, but also its moisture barrier properties. However, it is quite difficult to make a uniform blend of PLA pellets with starch/cellulose powders, especially at ambient temperature. Therefore, the use of powdered PLA instead of PLA pellets may facilitate the uniform mixing of PLA with starch/cellulose powders for the production of PLA-reinforced starch/cellulose composite foams. In this work, we are reporting a simple room-temperature mixing and high-temperature short-time compression moulding method for the development of cheap yet fully biodegradable starch/cellulose/PLA composite foams with substantially higher water barrier properties compared to the neat starch/cellulose composite foam that have the potential to replace the currently used EPS packaging. To the best of our knowledge, no published literature reported the enhancement of the water barrier properties and the flexural strength of starch/cellulose composite foam by the addition of PLA.

Table 1 The compositions of PLA-reinforced starch/cellulose composite foams.

Sample ID.	Dry weight (%)			
	Starch	Cellulose	PLA	Carnauba wax
Control	72.80	24.30	-	2.90
Composite 1	70.35	24.30	2.45	2.90
Composite 2	67.94	24.30	4.86	2.90
Composite 3	65.42	24.30	7.28	2.90

Composite 4	63.08	24.30	9.72	2.90

Experimental section

Materials

Potato starch and carnauba wax were procured from Earthpac Limited, New Zealand. The potato starch is composed of 28.6% amylose and 71.4% amylopectin, and it has an average granule size of 96 µm and approximately 16% moisture content. Cellulose fibre powder (500 to 800 µm long and 15 to 34 µm wide) was purchased from FineCel Sweden AB (Stockholm, Sweden). PLA powder was produced by cryogenic milling of PLA pellets (Ingeo 2003D, NatureWorks, USA, molecular weight M_n = 114317 g/mol measured by GPC) and the particle size was approx. 300 to 700 µm. The average size of the PLA powder was 500 µm.

Preparation of Starch/cellulose/PLA composite foams

Because of the difficulty of uniformly mixing of PLA pellets to starch/cellulose powders, the PLA pellets were ground to powder by a cryogenic mill (Model: 6870D, SPEX SamplePrep, LLC, Metuchen, USA). The weight (%) of cellulose fibre powder and carnauba wax was kept fixed but the weight (%) of PLA and starch were varied. Carnauba wax used as a plasticiser and internal mould release agent. A small quantity of water (145 ml) was added to obtain the

disruption of the native starch and to decrease the melt viscosity during compression moulding. Thermoplastic starch matrix behaviour varies depending on the formulations with a variation of glass transition temperature (Avérous et al. 2000). The processing stages begin with the dry blending of starch, cellulose fibre powder, and carnauba wax. Table 1 shows the compositions of various composite foams and the foam fabrication method is shown by a schematic diagram in Fig. 1. At the end of the mixing, a small amount of water was uniformly added to the starch/cellulose/carnauba wax mixture with continuous stirring and then the mixture was compression moulded to prepare the composite foams. They were mixed together at slow speed using a food mixer followed by the addition of water with continuous stirring to obtain a uniform granular mixture. The final moistened mixture was obtained after high speed mixing at 1500 rpm for 60 s.

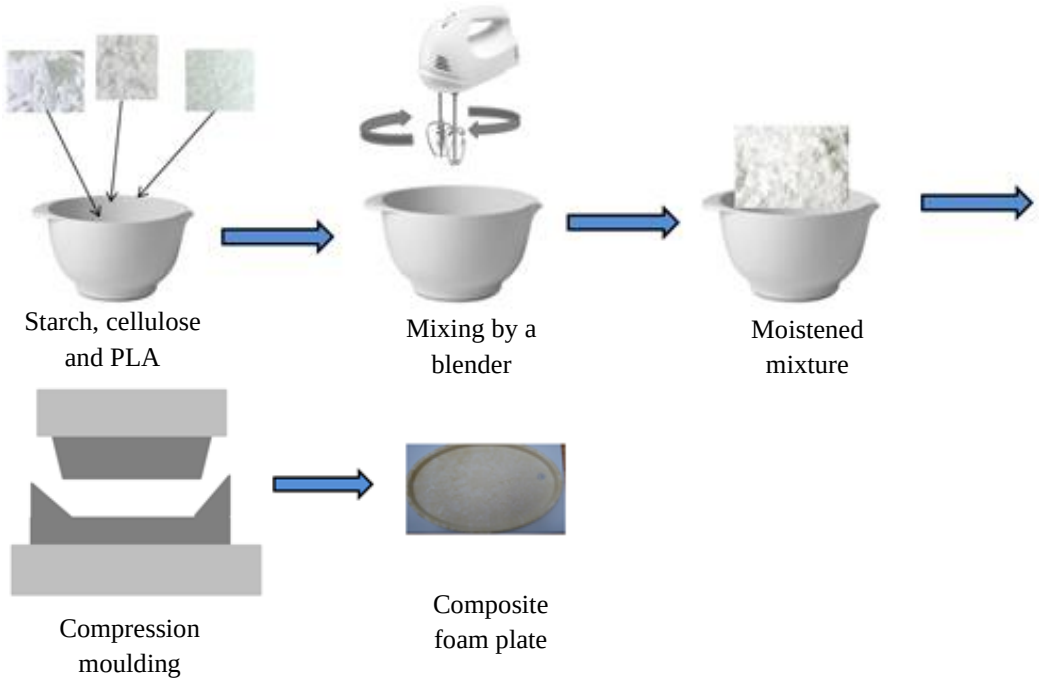

Fig. 1 The schematic diagram of PLA-reinforced starch/cellulose composite foam fabrication method.

85 g aliquot of the mixture was compression moulded in a plate-shaped mould at 220 °C for 60 s to convert the mixture into composite foam plates. The starches were quickly gelatinised and dry foam plates were produced by quick evaporation of water and volatiles during the compression moulding. To enhance the strength and the water barrier properties of potato starch/cellulose plates, PLA powder was added to the potato starch/cellulose mixture at 2.45, 4.86, 7.28 and 9.72 %. The foam composite samples were then cut into various sizes to carry out various characterisations.

Physicochemical and mechanical characterisations

The *CIE L*a*b** colour measurements of the starch/cellulose composite foams were carried out with a Mahlo spectrophotometer (Color eye 40/0, Mahlo GmbH, Germany) under D65 illuminant and 10° observer and the whiteness index was calculated according to the following equation:

$$Whiteness\ index = 100 - [(100 - L^*)^2 + (a^*)^2 + (b^*)^2]^{0.5} \quad (1)$$

Thermo-gravimetric analysis (TGA) was carried out in a TA Instruments' Discovery TGA (Model 550, TA Instruments Inc., New Castle, USA) from room temperature to 500 °C at a heating rate of 5 °C/min under nitrogen environment. 15 × 56 × 1.5 mm size samples with various PLA loadings were cut and dynamic mechanical thermal analysis (DMTA) was carried out in a 3-point static flexural mode using a dynamic mechanical analyser (Model RSA-G2, TA Instruments, New Castle, USA). The measurements were dynamic time sweep tests starting from T = 25 °C to 80 °C at a heating rate of 5 °C/min and frequency fixed at 1

Hz. The storage modulus (*E'*), loss modulus (*E''*), and loss factor (tan δ) of the samples were measured.

Specimens of 15.0 × 2.3 mm size were cut from the compression moulded starch/cellulose composite foams containing various PLA loading, and their tensile strength and elongation properties were measured by an Instron Universal Tensile Testing machine at a crosshead speed of 20 mm/min and gauge length of 30 mm at the standard atmospheric conditions (20±2 °C and 65±2% relative humidity). The flexural test was carried out according to the ASTM Test Method D 790-03 by a 3-point flexural test rig attached to an Instron Universal Tensile Testing machine at a crosshead speed of 2 mm/min at the standard atmospheric conditions (20±2 °C and 65±2% relative humidity) using a span length of 34.4 mm. The sample size was 60 × 20 × 2.5 mm and samples were preconditioned at the standard atmospheric conditions for 48 h before measuring. The vertical displacement was measured at the centre of the disc using an LVDT displacement transducer. For each sample, at least 10 tests were carried out and the averages are reported here. The flexural modulus was calculated according to the following equation:

$$E_{bend} = \frac{L^3 \times F}{4bh^3d} \qquad [1]$$

where, L = span length, F = force, b = sample width, h = sample thickness and d = difflection.

The contact angle was measured in dynamic mode by using a KSV CAM 100 Contact Angle Measurement Apparatus (KSV Instruments, Helsinki, Finland) and the Young-Laplace equation was used to quantify the contact angles. For each sample, the contact angle was measured at 5 places and the average contact angle was reported. The first measurement was taken immediately after placing a drop of water and then at 120 s interval measurements were taken until 480 s. The ordinary and the cracked surface of composite foams were

characterised by scanning the surface without any conductive coating in the backscattered mode on a Hitachi scanning electron microscope or SEM (Model: TM3030Plus, Hitachi Corporation, Japan) at an accelerating voltage of 15 kV.

The water absorption by a control starch/cellulose composite and also the composites containing various weight (%) of PLA was measured according to *ASTM Test Method D570: Standard Test Method for Water Absorption of Plastics*. 4 cm × 4 cm × 0.2 cm size samples were immersed in distilled water at room temperature after which they were removed from the tank after 10, 20, 30, 60, and 240 min, water adhered on the surface was wiped by a tissue paper and weighed. Finally, the water uptake was calculated as the mass difference, expressed as a percentage. The IR spectra of the composite foam surfaces were recorded using a PerkinElmer FTIR (Model: System 2000, PerkinElmer Corporation, USA) with an attenuated total reflectance (ATR) attachment using a Zn/Se ATR crystal. The fabric samples were placed flat on the upper side of the crystal. Good fibre to crystal contact was ensured by applying 50 N force using a calibrated torque wrench. 64 scans were carried out for each sample and the averages are reported here.

Results and discussion

Physical characteristics and colour

Fig. 2 shows the visual appearance of control starch/cellulose foam composite and also starch/cellulose composite foams containing various weight (%) of PLA. It can be seen that the surface of the composites are quite smooth with no visible pores. The colour of the

composites changed from yellowish with no PLA, to brownish with various weight (%) of PLA. The increase in PLA loading had a marginal effect in changing the colour of the starch/cellulose composite foams.

Table 2 shows the *CIE L*a*b** values and whiteness index of starch/cellulose composite foams containing various weight (%) of PLA. The colour of the foam composite started to become lighter and reddish with the addition of PLA as the value of *L** increased by the addition of PLA. The lightness value (*L**) of the control starch/cellulose foam composite was 93.54, which increased to 95.71 for the starch/cellulose composite foam containing 2.45% PLA. Further increase in the PLA loading had little effect on the value as its value was only slightly reduced. The addition of PLA initially increased the redness and decreased the yellowness of the composite. However, the redness (*a**) decreased and yellowness (*b**) increased with an increase in the PLA loading.

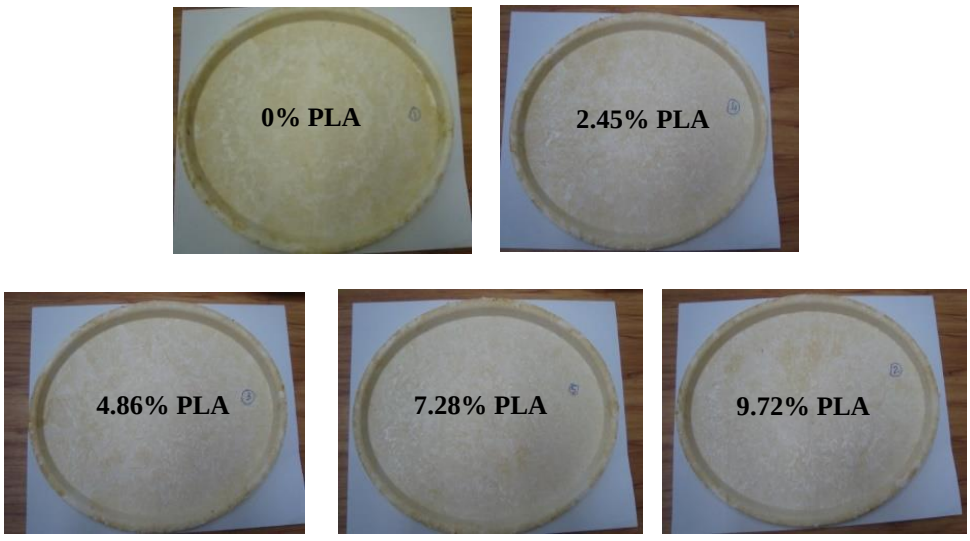

Fig. 2 Visual appearance of starch/cellulose composite foam plates with various PLA loading.

The control sample was more yellowish compared to the starch/cellulose composite foams with various PLA loadings. The addition of PLA to starch/cellulose foam composite increased its redness (*a**) but decreased the yellowness (*b**) up to 2.45% PLA loading but further increase in the PLA loading slightly decreased redness but increased the yellowness. It is evident that the addition of PLA had a marginal effect on the whiteness index of starch/cellulose composite foams as the whiteness index increased from 84.6 to 85.9 for the 0 to 2.45% PLA but the whiteness index decreased to 85.1 with an increase in the PLA loading.

Table 2 Colour and whiteness index of PLA-reinforced potato starch/cellulose composite foam s containing various PLA loading.

PLA loading (%)	*CIE*			Whiteness index
	L*	a*	b*	
0	93.54±0.15	1.15±0.10	13.97±0.11	84.60±0.08
2.45	95.71±0.07	1.9±0.03	13.29±0.15	85.90±0.10
4.86	95.56±0.08	1.98±04	13.65±0.08	85.50±0.05
7.28	95.37±0.12	1.88±0.06	13.84±0.12	85.30±0.05
9.72	95.02±0.05	1.82±0.03	13.89±0.11	85.10±0.03

Thermo-gravimetric analysis (TGA)

TGA was carried out to observe whether the addition of PLA has any effect on its thermal stability of the composite foams. As expected the weight loss of all starch/cellulose/PLA composite foams increased with an increase in the temperature due to the formation of

volatiles by the decomposition of the cellulose, starch, and PLA as shown in Fig. 3. Of the samples, neat PLA showed the best thermal stability but showed the lowest char yield. On the other hand, the starch/cellulose foam composite without any PLA showed the worst thermal stability. The addition of PLA to starch/cellulose composite foams improved the thermal stability of the composite foams, which improved with an increase in the weight (%) of PLA in the composite foams.

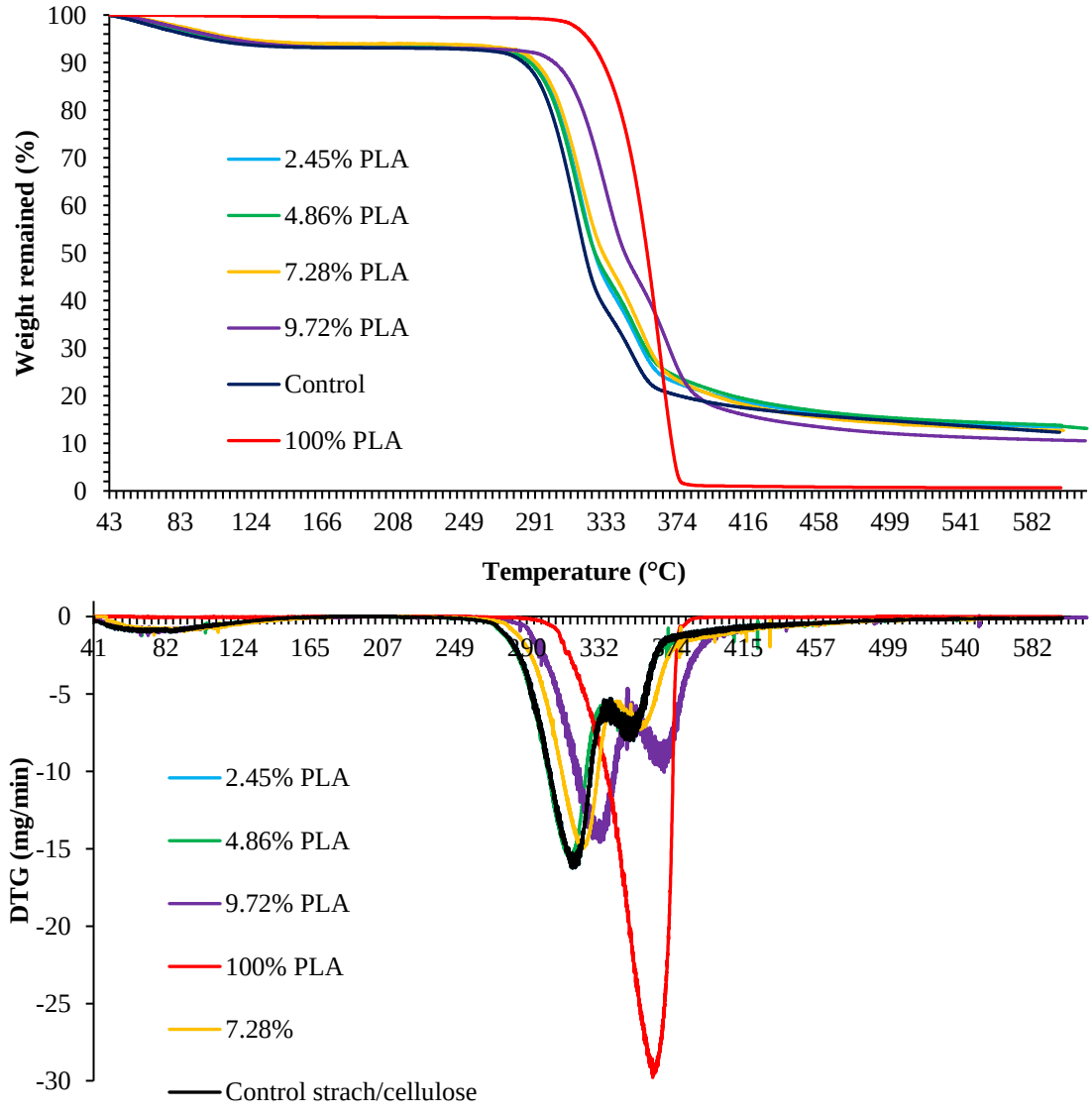

Fig. 3 Thermo-gravimetric (top) and DTG (bottom) curves of potato starch/cellulose composite foams containing various weight (%) of PLA.

It can be seen that for all samples the weight loss occurred at five stages: 60 – 120 °C, 120 – 278 °C, 278 – 327 °C, 327 – 362 °C, and 362 – 600 °C. The exception was the neat PLA for which the weight loss occurred at three stages: 60 – 305 °C, 305 – 380 °C, and 380 – 600 °C. For all composite samples, from room temperature to 320 °C, a small weight loss was observed but for neat PLA almost no weight loss was observed up to 277 °C; this is because PLA absorbs no moisture, whereas starch and cellulose both absorb moisture. The weight loss occurring in the composite samples in the 60 to 120 °C region is likely due to the loss of absorbed moisture (Orue et al. 2016), which decreased with an increase in the PLA loading. At 120 – 277 °C, the least weight loss was observed for all composite samples and less than 3% weight was lost at this stage.

Fig. 3 (bottom) shows the DTG curves of neat starch/cellulose foam and also composite foams with various PLA loadings. For all composite foams, the maximum degradation occurred in the temperature range of 278 to 327 °C, where approximately 65% weight loss was observed. For the control starch/cellulose foam composite the maximum degradation occurred at 315.65 °C, which increased to 316.4, 116.9, 319.5 and 320 °C for the starch/cellulose composites with 2.45, 4.86, 7.28 and 9.72% PLA loadings. The second highest degradation of the control composite occurred at 349 °C, which increased to 349.6, 351.7, 356.3 and 357.1 °C for the PLA loading 2.45, 4.86, 7.28 and 9.72% respectively. In contrast, the maximum degradation of PLA occurred at 363 °C. The rapid weight loss was observed in this stage due to depolymerisation and degradation of cellulose, starch, and PLA producing volatile compounds including carbon dioxide and carbon monoxide. The highest weight loss was observed for the neat PLA as the weight loss increased from 0.6% to 97.2% at 375 °C.

Dynamic mechanical thermal analysis (DMTA)

DMTA was carried out to determine the effect of the addition of PLA to the starch/cellulose composite foams had on their storage modulus (*E'*) and loss modulus (*E''*) at various temperatures, and also to understand their viscoelastic behaviour. Fig. 4 represents the storage modulus (*E'*) and loss modulus (*E''*) curves of starch/cellulose composite foams containing various weight percentage of PLA from room temperature to 200 °C. It is evident that for all the composite samples the storage modulus decreased with an increase in the temperature due to the loss of stiffness of the composite materials.

The control and the starch/cellulose sample containing 4.86% PLA had the highest stiffness at all temperatures. The composite containing 2.45% PLA also showed marginally higher storage modulus up to 58 °C than the control composite foam, but beyond that temperature, the control starch/cellulose composite showed higher storage modulus up to the maximum tested temperature. We have to remember that the glass transition temperature of PLA is 58 °C, i.e. below 58 °C it shows glassy nature and after 58 °C, it shows the characteristics of rubber. Therefore, above 58 °C, compared to the control starch/cellulose composite foam, the PLA-loaded composite foams showed reduced stiffness and the stiffness decreased with the increased PLA loading. At 30 °C, the storage modulus of the control starch/cellulose composite foam was 8.15×10^2 MPa, which increased to 8.87×10^2 and 9.14×10^2 MPa for the composite foam containing 2.45 and 4.86% PLA respectively. However, further increase in PLA loading decreased the storage modulus to 7.69×10^2 MPa for the 9.72% PLA loading. Compared to this, the control sample showed storage modulus of 6.18×10^2 and 5.19×10^2 MPa 86 and 170 °C respectively. The corresponding values for the PLA with 2.45, 4.86, 7.28 and 9.72% PLA loadings were 6.03×10^2 and 5.00×10^2, 5.56×10^2 and 4.50×10^2, 5.09×10^2 and 4.06×10^2, and 3.56×10^2 MPa respectively. Overall, the storage modulus of starch/cellulose composites decreased with an increase in the PLA loading.

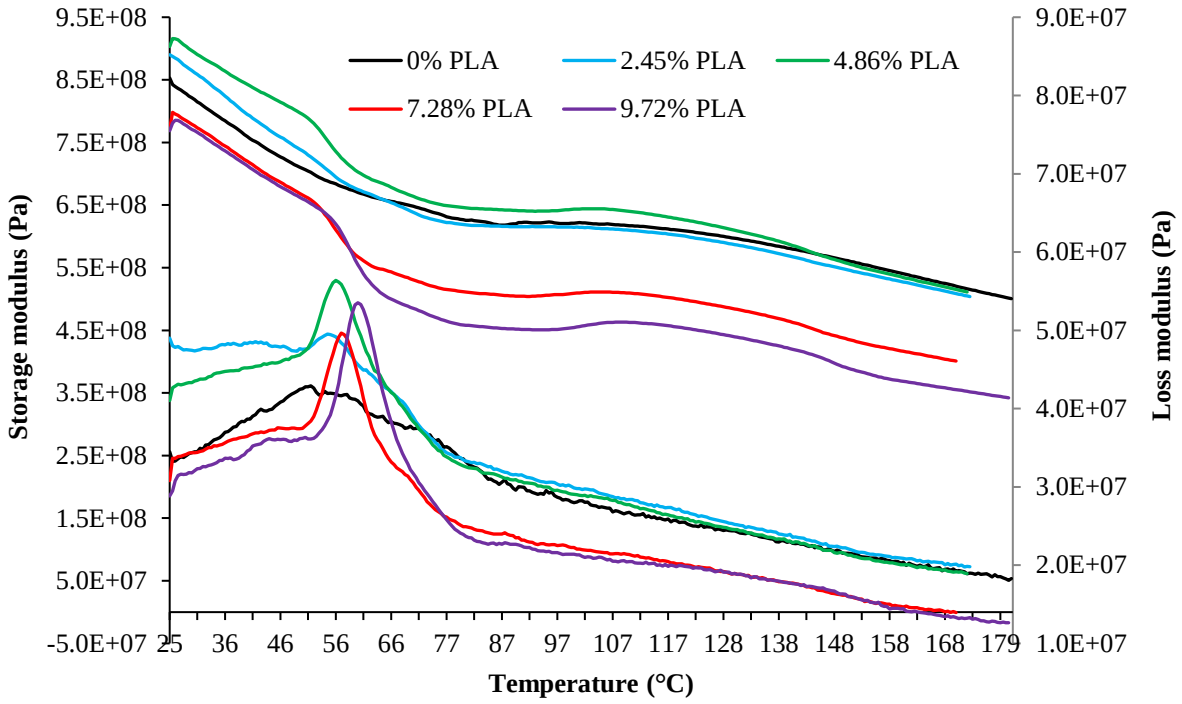

Fig. 4 Storage modulus and loss modulus of starch/cellulose composite foams containing various weight (%) of PLA at various temperatures.

The loss modulus accounts for the viscous component of the complex modulus or the out of phase component with the applied strain. The loss modulus also increased with an increase in the weight % of PLA up to 4.86% PLA loading, beyond which the loss modulus also decreased with an increase in the PLA loading. It can be concluded that the addition of PLA to starch/cellulose composites had a negative effect on their storage modulus at above 4.86% PLA loading.

The loss factor, Tan δ, is the ratio between the storage modulus and loss modulus, which represents mechanical damping or internal friction in a viscoelastic system. A high Tan δ value indicates that the material is inelastic, and a low value indicates that the material is elastic. The effect of adding PLA to the composites is expressed as a mechanical loss factor,

Tan δ, as a function of temperature (Fig. 5). The Tan δ curve peak, which is indicative of the glass transition temperature (T_g), is also indicative of the degree of crosslinking of the system. The control starch/cellulose composite does not show a sharp Tan δ peak, commonly associated with the T_g of a material, but rather shows a very broad peak, i.e. does not show any defined transition temperature. The starch/cellulose composites containing PLA had sharp Tan δ peaks. The starch/cellulose composite material containing 2.45% PLA shows a glass transition temperature of 58 °C, which increased to 60.8, 60.75 and 61.3 °C for the 4.86, 7.28 and 9.72% PLA, respectively. The composite containing 2.45% PLA showed glass transition temperature at 56 °C, which increased to 58 °C after PLA loading increased to 9.72%. The increase in peak height of Tan δ with an increase in the loading of PLA suggests that the stiffness of the starch/cellulose composite foam increased with PLA loading. The observed results are consistent with the results achieved by others (Avérous et al. 2001).

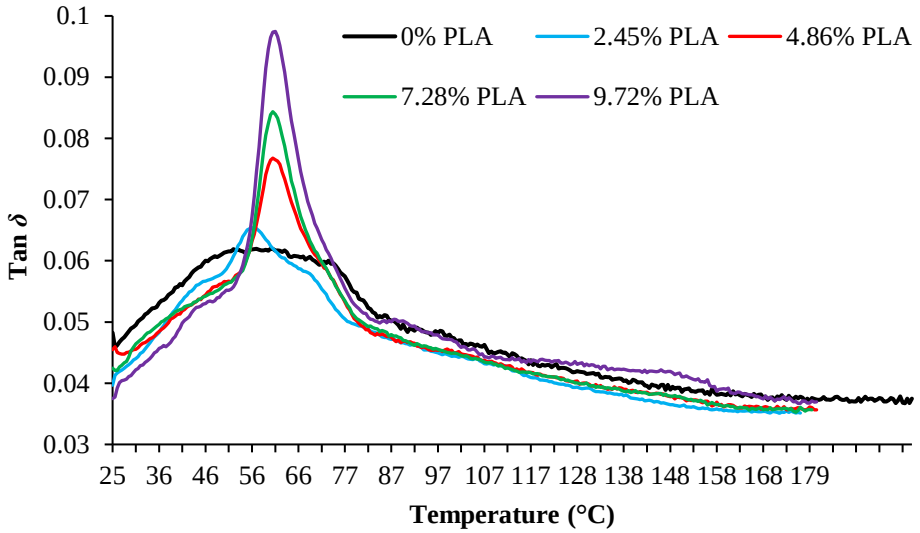

Fig. 5 The effect of increase of PLA loading on the Tan δ of the produced starch/cellulose composite foams as a function of temperature.

Effect of PLA loading on the mechanical properties of composites

The tensile strength and elongation properties were measured to assess whether the addition of PLA had any positive effect on their mechanical properties. Table 3 shows the tensile strength, breaking force and elongation at break of starch/cellulose composites containing various PLA loading. The addition of PLA to starch/cellulose composites had a positive

Table 3 Mechanical properties of starch/cellulose composites with various PLA loading.

PLA loading (%)	Tensile strength (MPa)	Elongation at peak (mm)	Breaking force (MPa)	Elongation at break (mm)
0	2.50	0.51	2.31	0.56
2.45%	2.70	0.58	2.59	0.63
4.86%	2.85	0.62	2.68	0.65
7.28%	2.99	0.68	2.79	0.67
9.72%	3.27	0.75	3.18	0.77

effect on their tensile strength and breaking force as these properties increased with an increase in the PLA loading. The tensile and breaking strengths of the control starch/cellulose foam composite were 2.50 and 2.31 MPa respectively, which increased to 3.27 and 3.18 MPa respectively for the foam composite containing 9.72% PLA, i.e. almost 31% increase in tensile strength. The results showed that the addition of PLA reinforced the composite foams.

Similarly, the elongation at peak and also elongation at break increased with an increase in the PLA loading.

Effect of PLA loading on the flexural properties of composites

The 3-point flexural test was carried out to observe whether the addition of PLA improves the rigidity/stiffness of the composite foam. In this test method, a test specimen is subjected to tension, compression, and shear simultaneously. The effect of PLA loading on the flexural or bending strength of starch/cellulose is presented in Fig. 6 (top). It can be seen that the addition of PLA to starch/cellulose had a positive effect on the flexural strength of the produced composite foam up to 4.86% PLA loading, after which the flexural strength started decreasing. The lowest flexural strength was observed for the starch/cellulose foam composites containing 4.86 and 9.72 % PLA as their flexural strength was even lower than the flexural strength exhibited by the control starch/cellulose foam. The flexural modulus exhibited by the control starch/cellulose foam composite was 345.91 KPa, which increased to 378.53 KPa for the 4.86% PLA loading; almost 9.43% increase in the bending rigidity. The increase in the flexural strength indicates that the adhesion between the matrix starch and PLA as well as between cellulose and PLA improved. Therefore, it can be concluded that the addition of PLA to the starch/cellulose composite had a reinforcing effect in increasing their flexural strength. It was reported that at 65% relative humidity, the tapioca starch foam and starch/PLA foam composites containing 10% PLA exhibited flexural strength of approximately 480 and 1080 KPa respectively [Preechawong et al., 2005]. However, in our case, the potato starch/cellulose composite foam showed only 345.91 KPa, which is considerably lower compared to the flexural strength showed by tapioca starch alone.

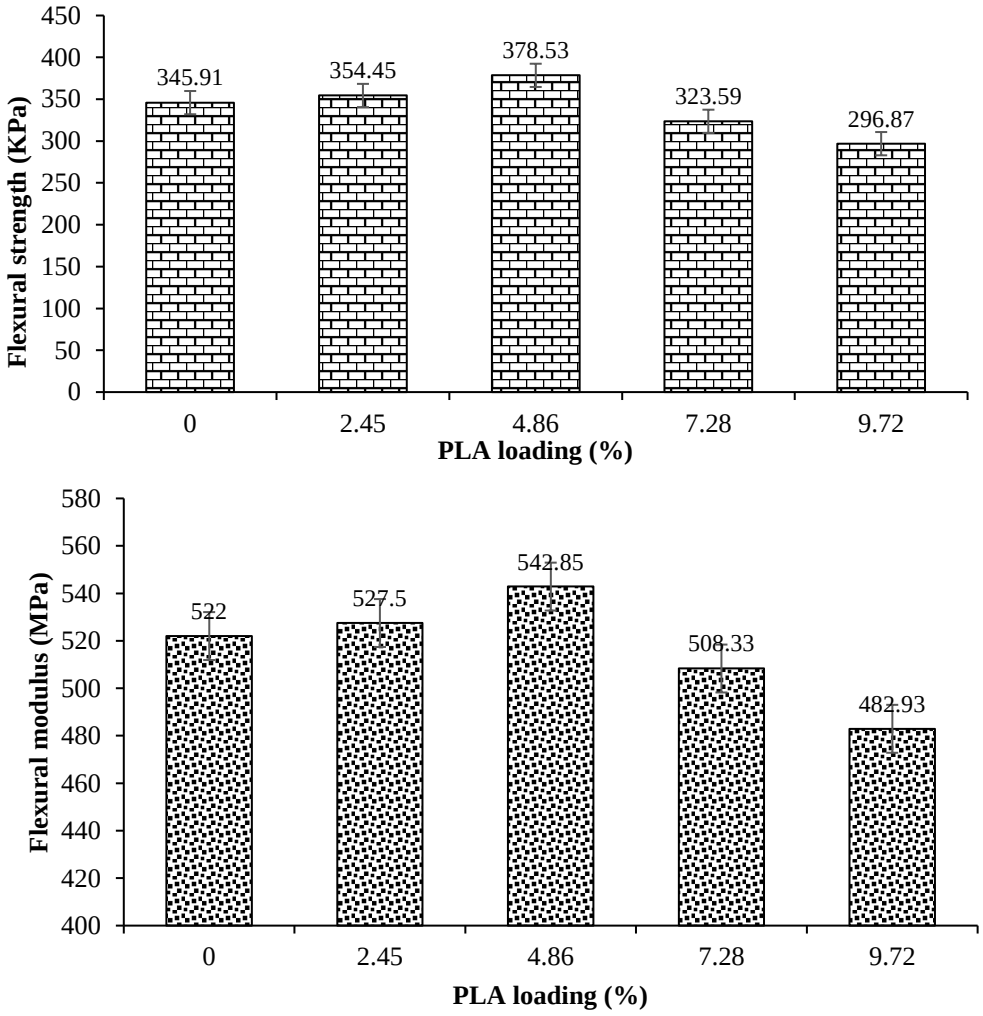

Fig. 6 Effect of increase of PLA loading on the flexural strength (top) and flexural modulus (bottom) of starch/cellulose composite foams.

Fig. 6 (bottom) shows the effect of PLA loading on the flexural modulus of the starch/cellulose composite foams. The addition of PLA to starch/cellulose foam composites at low PLA loading increased the flexural modulus of the starch/cellulose foam composites but increasing the PLA loading more than 4.86% resulted in decreased flexural modulus. The lowest flexural modulus was exhibited by the starch/cellulose composite containing 9.72%

PLA, which was 482.93 MPa. The flexural modulus exhibited by the starch/cellulose foam composite containing no PLA was 522.0 MPa, which increased to 527.5 and 542.85 MPa for the 2.45 and 4.86% PLA loading respectively, indicating that the composite containing 2.45 and 4.86% PLA was stiffer compared to the control starch cellulose composite. However, further increase in the PLA loading decreased the stiffness of the foam composites. The flexural modulus data shown in Fig. 6 are consistent with the storage modulus data shown in Fig. 2.

Cross-sectional and surface morphologies

The fractured surfaces of the composite foams were examined using scanning electron microscopy (SEM) to observe the effect of the addition of PLA on the microstructure (Fig. 7). The skin layer of all composites exhibited small, dense, and closed cell foam structure. However, the interior of the composite foams show quite large and opened cell structure. The size and distribution of the cells over the region are non-uniform. The dense outer skin layer was formed due to the abruption of evaporation of water molecules in the PLA-rich batter layer adjacent to the hot surface of mould [Preechawong et al., 2005]. The control starch/cellulose foam composite shows larger cells compared to the composites containing various weight (%) of PLA. In the interior of the composite foams, large opened cells were formed due to the rapid evaporation of a large amount of water during the high-temperature moulding, which expanded the pores before collapsing the pore walls during high-temperature moulding [Lawton et al., 1999]. The control starch/cellulose composite showed quite different morphologies compared to the starch/cellulose composites containing various weights (%) of PLA. The starch/cellulose composites containing 4.86 and 7.28% of PLA showed relatively uniform distribution of cells and uniform size of cells compared but

smaller cells than the control starch/cellulose composite. Starch/cellulose composite containing 9.72% of PLA showed some smaller cells but also some large cells, larger than the one observed for the control starch/cellulose composite foam. It is also evident that inside the starch/cellulose composite foams all starch granules were gelatinised as no starch granules are visible.

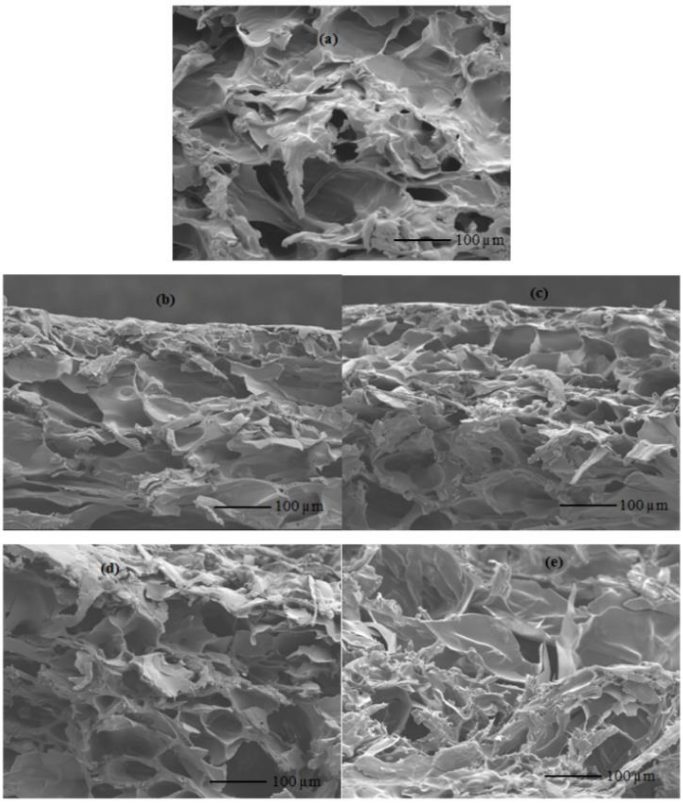

Fig. 7 SEM images of control starch/cellulose composite (a) and also starch/cellulose composite foams with 2.45 (b), 4.86 (c), 7.28 (d) and 9.72% (e) of PLA.

The SEM images of the surfaces of the starch/cellulose composite foams with increased loading of PLA are shown in Fig. S1 (Supplementary Material). The low magnified SEM images (left column of Fig. S1) show that in the case of 2.45% and 4.86% of PLA loading, hardly any PLA layer is visible on the surface of the composite foams as the PLA layer is

embedded into the starch/cellulose matrix. However, for higher PLA loading, some PLA layers are visible on the surface of the composite foams. At that PLA loading some PLA granules moved to the surface of the composites and at high moulding temperature they expanded forming layers of PLA. For the control sample, the cellulose fibre is visible on the surface. It is evident that some of the starch granules were not fully gelatinised during processing and did not expand but bonded to the rest of the fully gelatinised starch. The surface of the composite foams became smoother with increased loading of PLA, especially for 7.28 and 9.72% of PLA loading. PLA spread and covered the surface of composite foams as the moulding temperature used was considerably high and looked fully melted during the short moulding time. It is evident that for higher PLA loadings, PLA particles expanded forming thin layers that bonded to the gelatinised starch as shown in Fig. S1. Therefore, the foam composites with higher PLA loading showed increased flexural rigidity.

Dynamic contact angle

The water contact angle of composite foam was measured to determine whether the addition of PLA to the composites increases their surface hydrophobicity and water barrier properties. Fig. 8 shows the optical image of contact angle and water droplet shape at different times of surface of starch/cellulose composite foams having different PLA loading. From the dynamic water contact angle data of the surface of various composite foams, it is evident that the addition of PLA to starch/cellulose composites increased their hydrophobicity (Table S1 in Supplementary Material). It is expected that the surface of the control starch/cellulose composite would be hydrophilic as both starch and cellulose are strongly hydrophilic but it showed very low hydrophilicity. The control composite in these tests contains wax that

probably increased the hydrophobicity, which is evident in the high contact angle shown for the control.

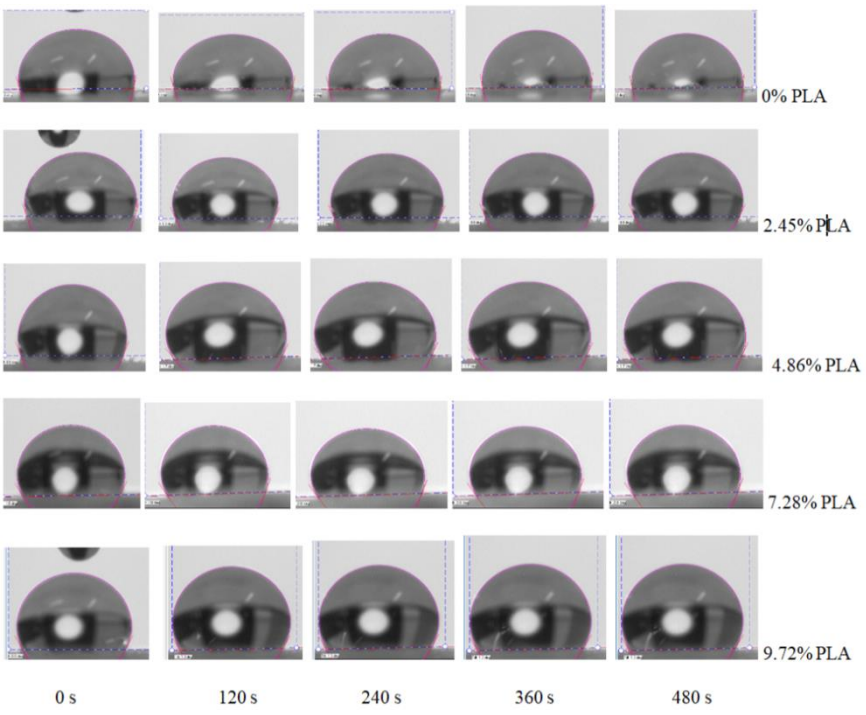

Fig. 8 Optical images of changing contact angle at different time for the surface of starch/cellulose composite foams containing various PLA loadings.

For the control starch/cellulose foam, the contact angle at 0 s was 102.3° that decreased to only 95.4° after 480 s showing some levels of hydrophobicity. The strong hydrogen bonding between hydroxyl groups of starch and cellulose along with carnauba wax might have contributed to increasing the hydrophobicity of the control starch/cellulose composite foam. On the other hand, the contact angle of the composite foams increased with an increase in the PLA loading and the contact angle was quite stable over 480 s indicating their excellent hydrophobicity. The composite foam with 9.72% PLA loading showed the highest contact angle (120.7°). The control starch/cellulose composite foam showed the lowest hydrophobicity as the contact angle decreased with time. The starch/cellulose composite

foam containing 9.72% showed the highest contact angle and it was stable until the end of test. The results indicate that the addition of PLA improved hydrophobicity or water barrier properties of the composite foams.

Water absorption

Water resistance of these samples was further investigated by carrying out a water absorption test. As expected, the control composite foam without PLA showed the highest absorption of water (Fig. S2 in Supplementary Material). The water absorption rate was highest in the first 10 min, after which the water absorption rate slowed but still showed an increase over time. All the other composites showed similar behaviour.

The composite foams containing 2.45, 4.86 and 7.28% PLA showed very similar water absorption but with an increase in time, considerable differences in water absorption were observed for the various weights (%) of PLA. The water absorption performance of starch/cellulose composites decreased with an increase in the weight (%) of PLA and the composite containing 9.72% PLA showed the lowest water absorption. The starch/cellulose composites containing 2.45, 4.86 and 7.28% PLA showed similar levels of water absorption but the composite containing 9.72% PLA showed considerably lower water absorption compared to the control starch/cellulose and other PLA containing composites. It can be concluded that the addition of PLA to the starch/cellulose composite had a positive effect in increasing their water barrier properties.

Attenuated Total Reflectance Fourier-transform infrared spectroscopy (ATR-FTIR)

The ATR-FTIR spectra of starch/cellulose composites containing PLA loadings are shown in Fig. S3 (Supplementary Material). The spectrum of control starch/cellulose composites shows characteristics bands of starch and cellulose at 758, 847, 930, 992, 1014, 1078, 1150, 1249, 2849, 2917, and broadband at 3255 cm^{-1}. The spectrum of control starch/cellulose composites shows four characteristic bands between 980 and 1160 cm^{-1} (992, 1014, 1078 and 1150 cm^{-1}) corresponding to the C−O bond stretching band attributed to primary alcohols (Marechal and Chanzy, 2000). The band at 1150 cm^{-1} can be assigned to the C−O−C asymmetric stretching vibrations, which shows that ether bonds were formed between the primary alcohol groups of starch resulting in a decrease in hydrophilicity. There is a new ester band formed at 1178 cm^{-1}, which came from the ester groups of PLA for the spectra of composites with PLA loading 4.86% and more, indicating the presence of PLA at the surface of the composite foams. The bands at 1315 and 1430 cm^{-1} can be assigned to CH_2 wagging symmetric bending and CH_2 asymmetric bending, respectively (Kacurakova et al. 2002). The absorption band at 1648 cm^{-1} is due to an intermolecular hydrogen bond involving the carboxyl groups. The bands at 2849 and 2917 cm^{-1} are due to symmetric and asymmetric C-H stretching vibrations. The broadband at 3255 cm^{-1} can be attributed to hydroxyl groups of starch and cellulose. The spectra of starch/cellulose composites containing various PLA loadings (%) show similar peaks but it is evident that the intensity of the broad hydroxyl peak at 3225 cm^{-1} decreased with an increase in the weight (%) of PLA. The reduction in the intensity of OH band indicates that the foam composite became more hydrophobic with an increase in the PLA loading in the composite foams.

Conclusions

We have demonstrated that the incorporation of PLA to starch/cellulose matrix modified the physical and chemical properties of starch-based composite materials bringing considerable improvements in water barrier properties, flexural strength, and flexural modulus. The addition of PLA to starch/cellulose composites slightly improved their thermal stability by increasing the peak thermal degradation temperature. The dynamic mechanical analysis results showed that the storage modulus of the composite gradually decreased with an increase in the weight (%) of PLA in the composite foams. The starch/cellulose composite foam did not show any glass transition temperature but the PLA containing foams showed glass transition temperature, which increased with an increase in the PLA loading. The peak height of tan δ increased with an increase in the weight (%) of PLA. The mechanical testing results show that the addition of PLA had a positive effect on the tensile strength, breaking force, and elongation at break of the composites. The 3-point bending test results showed that the bending strength of the starch/cellulose composites increased with the weight (%) of PLA. The SEM images confirmed that PLA showed quite good adhesion with gelatinised starch and cellulose, which caused the increased flexural strength and flexural rigidity shown by the composites low PLA loadings. The addition of PLA powder improved water absorption properties of the produced starch/cellulose composites may permit their application in packaging of foods or vegetables.

Acknowledgment This work was supported by the Ministry of Business, Innovation, and Employment (MBIE) of the Government of New Zealand (grant number BPLY1302) through the Biopolymer Network Ltd.

References

Abdel Rahman MA, Tashiro Y, Sonomoto K (2011) Lactic acid production from lignocellulose-derived sugars using lactic acid bacteria: Overview and limits. J Biotechnol 156:296–301.

Ali A, Xie F, Yu L, Liu H, Meng L, Khalid S, Chen L (2018) Preparation and characterization of starch-based composite films reinforced by polysaccharide-based crystals. Composites B 133:122–128.

Avérous L, Fringant C, Moro L (2001) Plasticized starch-cellulose interactions in polysaccharide composites. Polymer 42:6565–6572.

Avérous, L., Moro, L., Dole, P., Fringant, C. (2000). Properties of thermoplastic blends: starch-polycaprolactone. Polymer, 41, 4157–4167.

Carmona VB, De Campos A, Marconcini JM, Mattoso LHC (2014) Kinetics of thermal degradation applied to biocomposites with TPS, PCL and sisal fibres by non-isothermal procedures. J Therm Anal Calorim 115:153–160.

Chen J, Long Z, Wang J, Wu M, Wang F, Wang B, Lv W (2017) Preparation and properties of microcrystalline cellulose/hydroxypropyl starch composite films. Cellulose 24:4449–4459.

Corradini E, de Medeiros ES, Carvalho AJF, Curvelo AAS, Mattoso LHC (2006) Mechanical and morphological characterization of starch/zein blends plasticised with glycerol. J Appl Polym Sci 101:4133–4139.

Deng Y, Catchmark JM (2014) Insoluble starch composite foams produced through microwave expansion. Carbohydr Polym 111:864–869.

Dos Santos BH, De Souza Do Prado K, Jacinto AA, Da Silva Spinacé MA (2018) Influence of sugarcane bagasse fibre size on biodegradable composites of thermoplastic starch. J Renew Mater 6:176–182.

Edhirej A, Sapuan SM, Jawaid M, Zahari NI (2017) Cassava/sugar palm fibre reinforced cassava starch hybrid composites: Physical, thermal and structural properties. Int J Biologic Macromol 101:75–83.

Ghanbari A, Tabarsa T, Ashori A, Shakeri A, Mashkour M (2018) Preparation and characterization of thermoplastic starch and cellulose nanofibers as green nanocomposites: Extrusion processing. Int J Biologic Macromol 112:442–447.

Ghorpade VM, Gennadios A, Hanna MA (2001) Laboratory composting of extruded poly(lactic acid) sheets. Bioresour Technol 76:57–61.

Glenn GM, Orts WJ, Nobes GAR (2001a) Starch, fibre and $CaCO_3$ effects on the physical properties of foams made by a baking process. Ind Crop Prod 14:201–212.

Glenn GM, Orts WJ, Nobes GAR, Gray GM (2001b) In situ laminating process for baked starch-based foams. Ind Crop Prod 14:125–134.

Hietala M, Mathew AP, Oksman K (2013) Bionanocomposites of thermoplastic starch and cellulose nanofibers manufactured using twin-screw extrusion. Eur Polym J 49:950–956.

Ibrahim H, Mehanny S, Darwish L, Farag M (2017) A comparative study on the mechanical and biodegradation characteristics of starch-based composites reinforced with different lignocellulosic fibres. J Polym Environ 26:1–14.

Kacurakova M, Smith C, Gidley J, Wilson H (2002) Molecular interaction in bacterial cellulose composite studied by 1D FT-IR and dynamics 2D-FT-IR. Carbohydr Res 337:1145–1153.

Kaushik A, Singh M, Verma G (2010) Green nanocomposites based on thermoplastic starch and steam exploded cellulose nanofibrils from wheat straw. Carbohydr Polym 82:337–345.

Kim J-Y, Huber KC (2016) Preparation and characterization of corn starch-β-carotene composites, Carbohydr Polym 136:394–401.

Lawton JW, Shogren RL, Tiefenbacher KF (1999) Effect of batter solids and starch type on the structure of baked starch foams. Cereal Chem 76:682–687.

Liu D, Dong Y, Bhattacharyya D, Sui G (2017) Novel sandwiched structures in starch/cellulose nanowhiskers (CNWs) composite films. Compos Commun 4:5–9.

Marechal Y, Chanzy H (2000) The hydrogen bond network in I_β cellulose as observed by infrared spectrometry. J Molecular Struc 523:183–186.

Martin O, Schwach E, Avérous L, Couturier Y (2001) Properties of biodegradable multilayer films based on plasticized wheat starch. Stärke 53:372–380.

Mbey JA, Thomas F (2015) Components interactions controlling starch-kaolinite composite films properties. Carbohydr Polym 117:739–745.

Mendes JF, Paschoalin RT, Carmona VB, Sena Neto AR, Marques ACP, Marconcini JM, Mattoso LHC, Medeiros ES, Oliveira JE (2016) Biodegradable polymer blends based on corn starch and thermoplastic chitosan processed by extrusion. Carbohydr Polym 137:452–458.

Muller J, Jiménez A, González-Martínez C, Chiralt A (2016) Influence of plasticizers on thermal properties and crystallisation behaviour of Poly(lactic acid) films obtained by compression moulding. Polym Int 65:970–978.

Muneer F, Andersson M, Koch K, Menzel C, Hedenqvist MS, Gällstedt M, Plivelic TS, Kuktaite R (2015) Nanostructural morphology of plasticized wheat gluten and modified potato starch composites: relationship to mechanical and barrier properties. Biomacromolecules 16:695–705.

Noorbakhsh-Soltani SM, Zerafat MM, Sabbaghi S (2018) A comparative study of gelatin and starch-based nano-composite films modified by nano-cellulose and chitosan for food packaging applications. Carbohydr Polym 189:48–55.

Orue A, Corcuera MA, Pena C, Eceiza A, Arbelaiz A (2016) Bionanocomposites based on thermoplastic starch and cellulose nanofibers. J Thermoplast Compos Mater 29:817–832.

Patil NV, Netravali AN (2016) Microfibrillated cellulose-reinforced nonedible starch-based thermoset biocomposites. J Appl Polym Sci 133:43803.

Preechawong D, Peesan M, Supaphol P, Rujiravanit R (2005) Preparation and characterisation of starch/poly(L-lactic acid) hybrid foams. Carbohyd Polym 59:329–337.

Romero-Bastida CA, Tapia-Blácido DR, Méndez-Montealvo G, Bello-Pérez LA, Velázquez G, Alvarez-Ramirez J (2016) Effect of amylose content and nanoclay incorporation order in physicochemical properties of starch/montmorillonite composites. Carbohydr Polym 152:351–360.

Sagnelli D, Kirkensgaard JJK, Giosafatto CVL, Ogrodowicz N, Kruczał K, Mikkelsen MS, Maigret J-E, Lourdin D, Mortensen K, Blennow A (2017) All-natural bio-plastics using starch-beta-glucan composites. Carbohydr Polym 172:237–245.

Shirai MA, Grossmann MVE, Mali S, Yamashita F, Garcia PS, Müller CM) (2013) Development of biodegradable flexible films of starch and poly(lactic acid) plasticized with adipate or citrate esters. Carbohydr Polym 92:19–22.

Shogren RL, Lawton JW, Doane WM, Tiefenbacher KF (1998) Structure and morphology of baked starch foams. Polymer 39:6649–6655.

Spiridon I, Teacă C-A, Bodîrlău R, Bercea M (2013) Behaviour of cellulose reinforced cross-linked starch composite films made with tartaric acid modified starch microparticles. J Polym Environ 21:431–440.

Stepto RF (2006) Understanding the processing of thermoplastic starch. Macromol Sympos 245–246:571–577.

Subramaniam A (1990) Natural rubber. Ohm RF (Ed), The Vanderbilt Rubber Handbook. R.T. Vanderbilt Company, Norwalk,, USA, pp. 23–43.

Swanson CL, Shogren RL, Fanta GF, Imam SH (1993) Starch-plastic materials—Preparation, physical properties, and biodegradability (a review of recent USDA research). J Environ Polym Degrad 1:155–166.

Soykeabkaew N, Thanomsilp C, Suwantong O (2015) A review: Starch-based composite foams. Composites A 78:246–263.

Soykeabkaew N, Nittaya L, Atitaya N, Natthawut Y, Tawee T (2012) Reinforcing potential of micro- and nano-sized fibers in the starch-based biocomposites. Compos Sci Tech 72:845–52.

Soykeabkaew N, Supaphol P, Rujiravanit R (2004) Preparation and characterization of jute- and flax-reinforced starch-based composite foams. Carbohyd Polym 58:53–63.

Tabassi N, Moghbeli MR, Ghasemi I (2016) Thermoplastic starch/cellulose nanocrystal green composites prepared in an internal mixer. Iranian Polym J 25:45–57.

Wang P, Chen F, Zhang H, Meng W, Sun Y, Liu C (2017) Large-scale preparation of jute-fiber-reinforced starch-based composites with high mechanical strength and optimised biodegradability. Stärke 69:1700052.

Xu C, Chen C, Wu D (2018) The starch nanocrystal filled biodegradable poly (ε-caprolactone) composite membrane with highly improved properties. Carbohydr Polym 182:115–122.

Zhang C-W, Li F-Y, Li J-F, Wang L-M, Xie Q, Xu J, Chen S (2017) A new biodegradable composite with open cell by combining modified starch and plant fibres. Mater Design 120:222–229.

Zhou J, Song J, Parker R (2006) Structure and properties of starch-based foams prepared by microwave heating from extruded pellets. Carbohydr Polym 63:466–475.

Graphical abstract